# Inclusive and semi-inclusive polarized DIS data revisited

D. de Florian*
*Theoretical Physics, ETH Zürich CH-8093, Switzerland*

R. Sassot†
*Departamento de Física, Universidad de Buenos Aires, Ciudad Universitaria, Pab. 1 (1428) Bs.As., Argentina*

(Received 10 July 2000; published 11 October 2000)

We perform a combined next to leading order analysis of both inclusive and semi-inclusive polarized deep inelastic scattering data, assessing the impact of new data on the extraction of the sea quark and gluon spin dependent densities. In particular, we find that semi-inclusive data show a clear preference for a positive $\Delta\bar{u}$ distribution, although are almost insensitive to different alternatives to $\Delta\bar{d}$.

PACS number(s): 13.88.+e, 13.85.Qk

## I. INTRODUCTION

Over the last decade, there has been a remarkable improvement in our knowledge of the spin structure of the nucleon at the partonic level, driven by both the increase in precision and volume of data on spin dependent structure functions, and also on theoretical and phenomenological work around the ever increasing wealth of experimental evidence [1]. In the process, the extraction of spin dependent parton densities has evolved from mere extensions of simple scale independent *SU*(6)-inspired models, to consistent next to leading order (NLO) QCD global analysis based on a much more reduced set of model dependent hypotheses.

In spite of this significant progress, until very recently it was almost unavoidable to make rather crude assumptions about the way in which sea quarks are polarized or, more precisely, how polarization is distributed among the different sea quark flavors, the main reasons for this being the inability of totally inclusive data to discriminate between quarks and antiquarks, and the lack of enough statistics in the pioneering polarized semi-inclusive experiments. Because of these circumstances, up to now even the most refined global analyses have simply assumed polarization to be evenly distributed among the sea flavors, or in the most ambitious attempts, they have tried to discriminate between light and heavier flavors, but always in compliance with *SU*(2) isospin symmetry assumptions [2–5].

Motivated by the growing evidence supporting an SU(2) symmetry breaking between unpolarized sea quark distributions, more recently there has been a great deal of activity concerning sea quark polarization, including theoretical and phenomenological models advocating different degrees and realizations of *SU*(2) symmetry breakdowns [6], and even attempts to find evidence for them in the data [7].

Semi-inclusive asymmetries are sensitive to contributions coming from specific combinations of quarks of different flavor and nature, so in principle they can shed some light on the sea quark polarization issue. The theoretical framework needed to deal with them consistently up to NLO accuracy is well known [8], and indeed this kind of data was successfully included in a NLO global analysis some time ago [3]. However, the statistical weight of the data available at that time [9] hindered a significant impact on the parton distribution extraction. Since then, the Hermes Collaboration [10] have presented new semi-inclusive data with greater precision, a circumstance that justifies a new analysis taking into account also the new additions to the inclusive data set.

In this paper we perform a combined next to leading order analysis of both inclusive and semi-inclusive polarized deep inelastic scattering data, releasing the usual assumptions about flavor symmetry relations between the polarization of both valence and sea quarks, and we assess the role of semi-inclusive data in the experimental evaluation of these relations.

Performing this analysis we have found that semi-inclusive data constitute a clear constraint on the polarization of ''up'' antiquarks, information, which combined with that coming from inclusive measurements, fixes the polarization of valence quarks of the same flavor. However, ''down'' antiquark polarization remains loosely bounded, allowing a large uncertainty on ''down'' valence quark densities. As in previous analyses, the data imply a weak constraint on the polarized gluon density.

This paper is organized as follows: In Sec. II we review the framework for global analyses of inclusive and semi-inclusive data, and present our conventions. In Secs. III and IV we present the result for the fits to inclusive and combined (inclusive *plus* semi-inclusive) data, respectively. Finally, in Sec. V, we give our conclusions.

## II. CONVENTIONS AND FRAMEWORK

Throughout the present analysis we adopt the modified minimal subtraction ($\overline{\rm MS}$) factorization scheme, as implemented in our previous analysis [3], for writing inclusive and semi-inclusive asymmetries in terms of parton distributions up to NLO accuracy. For the inclusive asymmetries we take, as usual,

$$A_1^N(x,Q^2) \simeq \frac{g_1^N(x,Q^2)}{F_1^N(x,Q^2)}, \tag{1}$$

*Email address: dflorian@itp.phys.ethz.ch
†Email address: sassot@df.uba.ar

 

where the spin dependent structure function is given by

$$g_1^N(x,Q^2)=\frac{1}{2}\sum_{q,\bar{q}} e_q^2\left\{\Delta q(x,Q^2)+\frac{\alpha_s(Q^2)}{2\pi}\right.$$
$$\left.[\Delta C_q\otimes\Delta q+\Delta C_g\otimes\Delta g]\right\}, \qquad (2)$$

and in the case of three flavors can be alternatively written as

$$g_1^N(x,Q^2)=\left(\pm\frac{1}{12}\Delta q_3^{NS}+\frac{1}{36}\Delta q_8^{NS}+\frac{1}{9}\Delta\Sigma\right)$$
$$\otimes\left(1+\frac{\alpha_s}{2\pi}\Delta C_q\right)+\sum_q e_q^2\frac{\alpha_s}{2\pi}\Delta g\otimes\Delta C_g. \qquad (3)$$

In Eq. (3) the $\pm$ sign corresponds to either proton ($N=p$) or neutron ($N=n$) targets and

$$\Delta q_3^{NS}\equiv(\Delta u+\Delta\bar{u})-(\Delta d+\Delta\bar{d})$$
$$\Delta q_8^{NS}\equiv(\Delta u+\Delta\bar{u})+(\Delta d+\Delta\bar{d})-2(\Delta s+\Delta\bar{s})$$
$$\Delta\Sigma\equiv(\Delta u+\Delta\bar{u})+(\Delta d+\Delta\bar{d})+(\Delta s+\Delta\bar{s}). \qquad (4)$$

The first two (non-singlet) distributions evolve in $Q^2$ independently, whereas the gluon and the singlet distributions are coupled in the evolution.

It is worth noticing that whereas $\Delta q_3^{NS}$ can be obtained directly from data on the difference between the proton and the neutron spin dependent structure function $g_1^p-g_1^n$, the three remaining distributions that appear in Eq. (3) have to be obtained somewhat indirectly, i.e. exploiting their different scale dependence. Unfortunately, the limited amount of data available and the rather restricted range in $x$ and $Q^2$ covered do not allow one to do a precise determination of all the distributions. Nevertheless it should be kept in mind that even with an unbounded set of inclusive data of unlimited precision, it would only be possible to determine combinations of $\Delta q+\Delta\bar{q}=\Delta q_v+2\Delta\bar{q}$ (with $q=u,d,s$), but *never* $\Delta q_v$ and $\Delta\bar{q}$ separately, as can be seen from Eq. (4); therefore, the data are insensitive to the symmetry breaking in the sea sector.[1]

To be able to determine both $\Delta q_v$ and $\Delta\bar{q}$ one has to introduce some other independent input in the analysis, such as weak structure functions and Drell-Yan production, for which the theoretical framework is well known [11,12] but unfortunately there are no data yet or semi-inclusive deep inelastic scattering (SIDIS) asymmetries.

In order to perform the extraction of polarized valence and sea quark densities, we include SIDIS asymmetries measured by the Hermes and Spin Muon Collaborations (SMC), which are given by

$$A_1^{N\,h}(x,Q^2)|_Z\simeq\frac{\int_Z dz\, g_1^{N\,h}(x,z,Q^2)}{\int_Z dz\, F_1^{N\,h}(x,z,Q^2)}. \qquad (5)$$

There, the semi-inclusive analogue of $g_1^N$ is given by

$$g_1^{N\,h}(x,z,Q^2)=\sum_{q,\bar{q}} e_i^2\left\{\Delta q_i(x,Q^2)D_{q_i}^h(z,Q^2)+\frac{\alpha_s(Q^2)}{2\pi}[\Delta q_i\right.$$
$$\otimes\Delta C_{ij}\otimes D_{q_j}^h+\Delta q_i\otimes\Delta C_{ig}\otimes D_g^h+\Delta g\otimes\Delta C_{gj}$$
$$\otimes D_{q_j}^h]+\Delta M_{q_i}^h(x,z,Q^2)+\frac{\alpha_s(Q^2)}{2\pi}[\Delta M_{q_i}^h$$
$$\left.\otimes\Delta C_i+\Delta M_g^h\otimes\Delta C_g]\right\}, \qquad (6)$$

and $Z$ denotes the kinematical region covered by final state hadrons ($z_h=P\cdot h/P\cdot q>0.2$ in [9,10]). The first line in Eq. (6) represents the familiar LO contribution to semi-inclusive processes, the second accounts for current fragmentation up to NLO, and the third is associated with target fragmentation and can be neglected for the kinematical region explored by Hermes and SMC [13]. The full expressions for the coefficients in Eqs. (2) and (6) in the $\overline{\rm MS}$ can be found in [3] and references therein.

SIDIS data are available for different kinds of targets and species of hadrons identified in the final state ($p$, $D$, He and $\pi^\pm,h^\pm$ respectively). Since fragmentation functions depend strongly on the flavor of the originating parton and on the charge of the hadron, it is possible to construct alternative combinations of parton distributions which are independent of the ones contributing to the inclusive asymmetry. In this way, in principle it is possible to do a full flavor decomposition for the polarized parton distributions.

Fragmentation functions are obtained from fits to $e^+e^-\to h$ data and, similarly to what happens in inclusive DIS, those measurements allow only the determination of the combination $D_q^h+D_{\bar{q}}^h$. In order to construct the full set of fragmentation functions needed to analyze the SIDIS data for $h^+$ and $h^-$, one has to have some extra assumptions. In the present analysis we take into account only contributions from $\pi$'s and $K$'s, and for both mesons we define a $Q^2$ and flavor independent function[2] $\eta_D$, which allows one to separate between the ''favored'' and ''unfavored'' fragmentation functions for each flavor and final state hadron as

[1]In this sense, claims stating that ''the data tolerate strong flavor symmetry violations in the sea sector'' (as in Ref. [5]) are just rather void statements, since of course it is always possible to modify $\Delta\bar{q}$ in such a way that $\Delta q+\Delta\bar{q}$ remains unchanged.

[2]Therefore the $Q^2$ dependence of the ''favored'' and ''unfavored'' fragmentation functions is given, in our approximation, by the one of the total distributions fitted from $e^+e^-$ data.

$$D_u^{\pi^+}=D_{\bar{u}}^{\pi^-}=D_{\bar{d}}^{\pi^-}=D_d^{\pi^+}\equiv D_1^{\pi}=(D_u^{\pi^+}+D_{\bar{u}}^{\pi^+})\frac{1}{1+\eta_D}$$

$$D_u^{\pi^-}=D_{\bar{u}}^{\pi^+}=D_{\bar{d}}^{\pi^+}=D_d^{\pi^-}\equiv D_2^{\pi}=(D_u^{\pi^+}+D_{\bar{u}}^{\pi^+})\frac{\eta_D}{1+\eta_D}$$

$$D_s^{\pi^-}=D_{\bar{s}}^{\pi^+}=D_s^{\pi^+}=D_{\bar{s}}^{\pi^-}\equiv\frac{1}{2}(D_s^{\pi^+}+D_{\bar{s}}^{\pi^+}) \tag{7}$$

and

$$D_u^{K^+}=D_{\bar{u}}^{K^-}=D_{\bar{s}}^{K^-}=D_s^{K^+}\equiv D_1^{K}=(D_u^{K^+}+D_{\bar{u}}^{K^+})\frac{1}{1+\eta_D}$$

$$D_u^{K^-}=D_{\bar{u}}^{K^+}=D_{\bar{s}}^{K^+}=D_s^{K^-}\equiv D_2^{K}=(D_u^{K^+}+D_{\bar{u}}^{K^+})\frac{\eta_D}{1+\eta_D}$$

$$D_d^{K^-}=D_{\bar{d}}^{K^+}=D_d^{K^+}=D_{\bar{d}}^{K^-}\equiv\frac{1}{2}(D_d^{K^+}+D_{\bar{d}}^{K^+}). \tag{8}$$

In agreement with measurements of *unpolarized* SIDIS data [15], we parametrize $\eta_D$ as

$$\eta_D(z)=a\frac{1-z}{1+z}. \tag{9}$$

The usual Field-Feynman parametrization for $\eta_D$ [14] corresponds to Eq. (9) with $a$ set to 1. In our case we will vary the parameter $a$ around the default value of 1, as a way to quantify the uncertainties introduced by the assumptions on the fragmentation functions in the extracted polarized parton distributions.

Regarding the normalization of Eqs. (1) and (5), it is customary to write the unpolarized structure functions $F_1^N(x,Q^2)$ in terms of the more familiar $F_2^N(x,Q^2)$:

$$F_1(x,Q^2)=\frac{F_2(x,Q^2)}{2x}\frac{[1+\gamma^2(x,Q^2)]}{[1+R(x,Q^2)]}, \tag{10}$$

where $\gamma^2(x,Q^2)=4M^2x^2/Q^2$, $R(x,Q^2)$ is the ratio between the longitudinal and transverse photoabsortion cross sections, and we have dropped the nucleon target label $N$. Therefore, the asymmetry for inclusive data is given by

$$A_1(x,Q^2)=\frac{g_1(x,Q^2)}{F_2(x,Q^2)}\frac{2x[1+R(x,Q^2)]}{[1+\gamma^2(x,Q^2)]}, \tag{11}$$

and similarly for the semi-inclusive one.

The information on the polarized parton distributions, whose extraction is the goal of the global fit, is therefore fully contained in the polarized structure function $g_1(x,Q^2)$, which can be reconstructed using the known (measured or computed) values of $A_1(x,Q^2)$, $F_2(x,Q^2)$ and $R(x,Q^2)$.

Of course, the $A_1(x,Q^2)$ values are obtained from measurements, but there is still some freedom in taking $F_2$ and $R$, i.e. either from experimental data or from perturbative QCD (PQCD) calculations. Since both quantities are strongly affected by higher twist contributions and unknown higher order corrections in the measured range of $x$ and $Q^2$, but only a leading twist LO or NLO expression for $g_1$ is used in Eq. (11) under the assumption that higher twist effects may cancel when taking the ratio, in the past it has been considered more consistent from the perturbation theory point of view to use the PQCD result for both $F_2$ and $R$.

On the other hand, it is worth noticing that the measured quantity in polarized DIS is $A_{\|}$, related to $A_1$ by

$$A_{\|}=D(A_1+\eta A_2)\sim DA_1, \tag{12}$$

where the depolarization factor $D$ is obtained from the *measured value* of $R$. Furthermore, it turns out that the effect of using either $R_{expt}$ or $R_{QCD}$ can represent a difference up to 20% (40%) at NLO (LO) for the smallest values of measured $x$, and still persists, although becomes smaller, even for values of $x$ and $Q^2$ where higher twist effects are expected to be small (like for SMC data). An analogous effect is expected in $F_2$; however, in this case the differences are found to be smaller.

In our analysis we have decided to use the experimental value of $R$ from Ref. [16] in order to be consistent with the extraction of $A_1$ from $A_{\|}$, but still construct $F_2$ using the PQCD expressions that can be obtained from the unpolarized analogue of Eqs. (2) and (6) and the 1998 Glück-Reya-Vogt (GRV98) [17] set of unpolarized parton distributions. The choice for a perturbative $F_2$ is forced by the fact that our fit is also performed to semi-inclusive data, and thus we need consistency between the normalization of inclusive and semi-inclusive asymmetries. For the time being no experimental values of $F_2^h$ are available for the normalization of the latter, at least for the same bins of $x$ and $Q^2$ measured by SMC and Hermes. Regarding $R_{expt}^h$, we have just assumed that the same value applies for both inclusive and semi-inclusive data. Fragmentation functions were taken from [18].

Clearly, the extraction of $R^h$ and $F_2^h$ from unpolarized semi-inclusive data will be a great advantage in the future in order to perform a fully consistent analysis. Nevertheless, as we have stated before, there are still some other uncertainties in the semi-inclusive case which are expected to hinder the ones coming from eventual differences between $R$ and $R^h$.

We also implement a different strategy to that used in [3] for parametrizing and extracting parton densities. The procedure consists of two stages. The first stage is the one in which totally inclusive data are used to fix the net polarization carried by each quark flavor, but without discriminating between quarks and antiquarks, as this distinction is beyond the reach of this kind of data. For $u$ and $d$ quarks *plus* antiquarks densities at the initial scale $Q_0^2=0.5$ GeV$^2$ we propose

$$x(\Delta q+\Delta\bar{q})=N_q\frac{x^{\alpha_q}(1-x)^{\beta_q}(1+\gamma_q x^{\delta_q})}{B(\alpha_q+1,\beta_q+1)+\gamma_q B(\alpha_q+\delta_q+1,\beta_q+1)}, \tag{13}$$

while for strange quarks *plus* antiquarks we use

TABLE I. Inclusive and semi-inclusive data used in the fit.

| Collaboration | Target | Final state | No. points | Refs. |
|---|---|---|---|---|
| EMC | Proton | Inclusive | 10 | [21] |
| SMC | Proton, deuteron | Inclusive | 12, 12 | [22] |
| E-143 | Proton, deuteron | Inclusive | 82, 82 | [23] |
| E-155 | Proton, deuteron | Inclusive | 24, 24 | [24] |
| Hermes | Proton, helium | Inclusive | 9, 9 | [10] |
| E-142 | Helium | Inclusive | 8 | [25] |
| E-154 | Helium | Inclusive | 17 | [26] |
| SMC | Proton, deuteron | $h^+$, $h^-$ | 24, 24 | [9] |
| Hermes | Proton, helium | $h^+$, $h^-$ | 18, 18 | [10] |

$$x(\Delta s+\Delta\bar{s})=2N_s\frac{x^{\alpha_s}(1-x)^{\beta_s}}{B(\alpha_s+1,\beta_s+1)}, \tag{14}$$

with a similar parametric form for gluons:

$$x\Delta g=N_g\frac{x^{\alpha_g}(1-x)^{\beta_g}}{B(\alpha_g+1,\beta_g+1)}. \tag{15}$$

The first moments of the quark densities $\delta q$ ($N_q$) are often related to the hyperon beta decay constants $F$ and $D$ through the $SU(3)$ symmetry relations

$$\delta u+\delta\bar{u}-\delta d-\delta\bar{d}\equiv N_u-N_d=F+D\equiv 1.2573 \tag{16}$$

$$\delta u+\delta\bar{u}+\delta d+\delta\bar{d}-2(\delta s+\delta\bar{s}) \equiv N_u+N_d-4N_s=3F-D\equiv 0.579. \tag{17}$$

Under such an assumption, the previous equations would strongly constrain the normalization of the quark densities. However, as we are interested also in testing flavor symmetry at different levels, we leave aside that strong assumption and relax the symmetry relations introducing two parameters, $\epsilon_{Bj}$ and $\epsilon_{SU(3)}$ respectively. These parameters account quantitatively for eventual departures from flavor symmetry considerations, including also some uncertainties in the low-$x$ behavior and higher order corrections

$$N_u-N_d=(F+D)(1+\epsilon_{Bj}) \tag{18}$$

$$N_u+N_d-4N_s=(3F-D)(1+\epsilon_{SU(3)}), \tag{19}$$

and we take them as a measure of the degree of fulfillment of the Bjorken sum rule [19] and the $SU(3)$ symmetry [20].

Equations (18) and (19) allow us to write the normalization of the three quark flavors in terms of $N_s$, $\epsilon_{Bj}$, and $\epsilon_{SU(3)}$. Notice that no constraints have been imposed on the breaking parameters since we expect them to be fixed by the data. The remaining parameters are constrained in such a way that positivity with respect to GRV98 parton distributions is fulfilled. This is particularly relevant at large $x$, and since no polarized data are available in that kinematical region, we directly fix the parameters $\beta_u=3.2\,(3.05)$, $\beta_d=4.05\,(3.77)$ and $\beta_g=6\,(6)$ for the NLO (LO) sets in agreement with GRV98. Consistently with the choice for the unpolarized parton distributions, we use the values of $\Lambda_{QCD}$ given in Ref. [17] to compute $\alpha_s$ at LO and NLO.

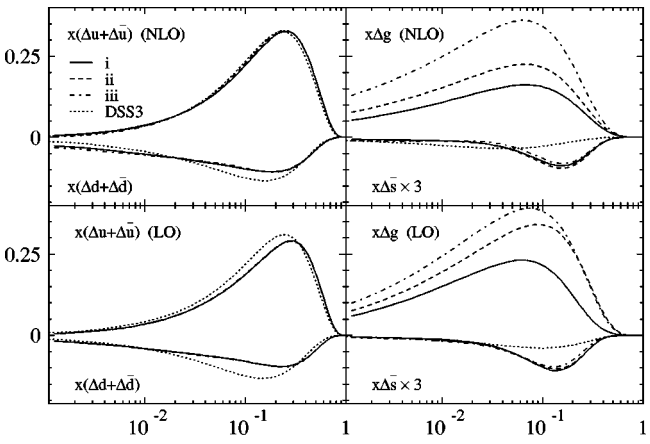


FIG. 1. LO and NLO polarized parton densities from inclusive data at $Q^2=10$ GeV$^2$.

In this way, in the first stage we obtain from the inclusive data set all the information available there without any unnecessary symmetry assumptions. The second stage of the procedure incorporates semi-inclusive data in order to extract antiquark densities, and consequently to fix valence quark densities, relying on the possibility to discriminate between quarks and antiquarks given by positive and negatively charged hadron production asymmetries. As antiquark densities we take

$$x\Delta\bar{q}=N_{\bar{q}}\frac{x^{\alpha_{\bar{q}}}(1-x)^{\beta_s}}{B(\alpha_{\bar{q}}+1,\beta_{\bar{q}}+1)}, \tag{20}$$

for $\bar{u}$ and $\bar{d}$ quarks, and we assume $\bar{s}=s$ since the possibility of discrimination in the $s$ sector is beyond the precision of the data and $\beta_{\bar{q}}=\beta_s$.

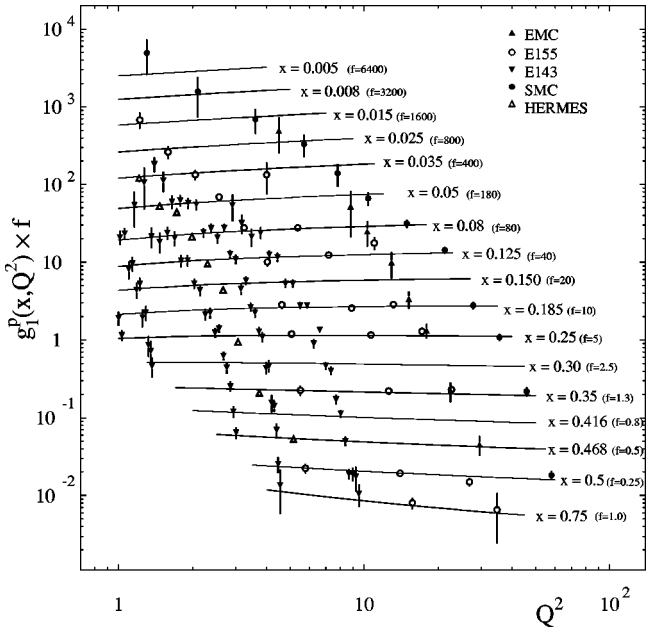


FIG. 2. $g_1$ data against NLO inclusive set (i).

TABLE II. First moments for LO and NLO distributions at $Q^2=10$ GeV$^2$.

| Set | | $\chi^2_I$ | $\epsilon_{Bj}$ | $\epsilon_{SU(3)}$ | $\delta u+\delta\bar{u}$ | $\delta d+\delta\bar{d}$ | $\delta s$ | $\delta g$ | $\delta\Sigma$ |
|---|---|---|---|---|---|---|---|---|---|
| NLO | (i) | 228.66 | −0.015 | −0.003 | 0.780 | −0.458 | −0.064 | 0.75 | 0.194 |
| | (ii) | 228.69 | −0.018 | 0.037 | 0.776 | −0.458 | −0.071 | 1.07 | 0.175 |
| | (iii) | 230.33 | −0.002 | −0.063 | 0.767 | −0.486 | −0.066 | 1.75 | 0.15 |
| LO | (i) | 237.55 | −0.126 | 0.016 | 0.713 | −0.385 | −0.065 | 0.88 | 0.199 |
| | (ii) | 236.10 | −0.126 | 0.018 | 0.708 | −0.39 | −0.068 | 1.4 | 0.181 |
| | (iii) | 236.44 | −0.126 | 0.009 | 0.702 | −0.396 | −0.069 | 1.68 | 0.169 |

The data sets analyzed in both stages include only points with $Q^2>1$ GeV$^2$ listed in Table I, and totaling 137, 118, and 34 points, from proton, deuteron, and helium targets respectively, in the inclusive stage, plus 42, 24, and 18, from proton, deuteron, and helium targets respectively, in the second stage. In order to take into account correlations between inclusive and semi-inclusive measurements, we only analyze the inclusive data for SMC and Hermes for ''averaged'' bins. In the semi-inclusive case we take into account in the fit only the most precise data concerning the production of charged $\pm$ hadrons (without identifying pions, kaons, or other particles individually).

## III. INCLUSIVE DATA

In this section we present the results coming from the analysis of the inclusive data set. Taking into account that in previous analyses, even those which have used most recent inclusive data, the gluon densities have been found to be rather poorly constrained, we extract three different sets with the gluon first moment constrained to be lower than 0.4 and labeled as (i), bounded between 0.4 and 0.7 and denoted as (ii), and greater than 0.7 labeled as (iii), respectively, at the initial scale. Doing this, we aim to explore different regions for gluon polarization and, at the same time, to provide different scenarios for predictions in future experiments. As we will show, data prefer gluon distributions with first moments around those values but does not really constrain them in a precise way.

The resulting densities from the LO and NLO analysis, and the corresponding relevant features at 10 GeV$^2$, are shown in Fig. 1 and Table II, respectively. The corresponding parameters are given in Table VII.

Even though the precision attained by these kind of fits is remarkable good, as shown in Fig. 2, there seems to be a slight systematic discrepancy between the Hermes data and the results of the remaining experiments. For these reasons, in the fitting procedure we have applied to the Hermes data a normalization factor which we allow to depart from unity up to a 5% (it saturates at the upper limit), without almost any consequences in the obtained parton distributions, but with a significant improvement in the $\chi^2$ values.

As can be seen in Fig. 1 the three sets have rather large differences in the gluon distribution (with a very mild preference for set (i) at NLO and (ii) at LO), with close results for the net polarization of each quark flavor. The quality of the fits is comparable; in fact, it is hard to distinguish between the inclusive asymmetries estimates coming from these sets. As it is shown in Table II, the differences in $\chi^2$ are rather small, and allowing variations within just two units, it is possible to go from an almost negligible polarized gluon distribution to a highly polarized one. The reason for this can be easily understood from Fig. 2, where all proton data for $g_1$ are shown as a function of $Q^2$. DIS data, in principle, constrain the gluon distribution through the evolution of $g_1$, but unfortunately, available data do not show a real lever arm in $Q^2$, particularly at lower values of $x$ where the gluon density is expected to drive the evolution.

Even though available data indicate that $\delta g(Q^2=10)\sim 1\pm 1$ (see Altarelli *et al.* in Ref. [2] for a more exhaustive analysis), we clearly have to wait for less inclusive data as in jet [27], prompt photon [28], and heavy quark [29] production to be able to determine the distribution with a reasonable precision.

In Fig. 1 we have included also $u$, $d$, and $s$ distributions obtained in our previous analysis (de Florian–Sampayo–Sassot (DSS) fit 3) [3]. As can be observed, the differences in the $u$ and $d$ distributions are rather small, and although there are some additions of new data in the analysis, they mainly originate in the use of the experimental value of $R$ instead of the perturbative one as was done in our previous analysis. This is particularly manifest in the LO case, where the perturbative approach yields $R=0$.

It is also worth remarking that the fits prefer $d$ distributions steeper at small $x$ than the $u$ ones, i.e. $\alpha_d<\alpha_u$. Since there are almost no neutron data able to constrain $\Delta d+\Delta\bar{d}$ at $x<0.01$, this effect should rather be considered as a result of the extrapolation of the distributions than as experimental evidence of $g_1^n$ being steeper than $g_1^p$. Clearly, more precise neutron and deuteron data at small $x$ would help to clarify this feature.

TABLE III. First moment of $g_1^{p-n,p,n}$ at $Q^2=10$ GeV$^2$.

| Set | | $\Gamma^{Bj}$ | $\Gamma_1^p$ | $\Gamma_1^n$ |
|---|---|---|---|---|
| NLO | (i) | 0.191 | 0.130 | −0.061 |
| | (ii) | 0.191 | 0.129 | −0.062 |
| | (iii) | 0.194 | 0.126 | −0.067 |
| LO | (i) | 0.183 | 0.130 | −0.053 |
| | (ii) | 0.183 | 0.128 | −0.055 |
| | (iii) | 0.183 | 0.126 | −0.057 |

TABLE IV. $\chi^2$ of the LO and NLO fits and the first moment of the distributions obtained from the combined analysis at $Q^2=10$ GeV$^2$.

| | Set | $\chi^2_T$ | $\delta u_V$ | $\delta d_V$ | $\delta\bar{u}$ | $\delta\bar{d}$ |
|---|---|---|---|---|---|---|
| NLO | (i+) | 330.52 | 0.649 | −0.576 | 0.063 | 0.061 |
| | (i−) | 330.00 | 0.686 | −0.357 | 0.045 | −0.049 |
| | (ii+) | 330.98 | 0.656 | −0.555 | 0.058 | 0.056 |
| | (ii−) | 330.22 | 0.684 | −0.357 | 0.043 | −0.046 |
| | (iii+) | 332.31 | 0.652 | −0.583 | 0.055 | 0.053 |
| | (iii−) | 331.64 | 0.679 | −0.392 | 0.041 | −0.044 |
| LO | (i+) | 336.24 | 0.599 | −0.493 | 0.060 | 0.060 |
| | (i−) | 335.54 | 0.629 | −0.291 | 0.043 | −0.043 |
| | (ii+) | 334.19 | 0.592 | −0.498 | 0.058 | 0.058 |
| | (ii−) | 334.03 | 0.624 | −0.295 | 0.042 | −0.042 |
| | (iii+) | 334.26 | 0.591 | −0.490 | 0.056 | 0.056 |
| | (iii−) | 333.69 | 0.624 | −0.298 | 0.041 | −0.041 |

Finally, the most prominent difference between the results of the present analysis and those from DSS is the one found between the strange spin dependent distributions. Even though their first moments are both negative and rather close in magnitude, the shape of the distributions differs, mainly because $\Delta s$ is not bounded to obey the $SU(3)$ symmetric relations within the sea, the constraint that was applied in the DSS analysis [3]. This difference gives also an idea of the large uncertainties in this distribution, which is clearly not well constrained by the available data.

Regarding the symmetry breaking for inclusive data, it is worth noticing that for the three NLO sets the Bjorken sum rule breaking parameter $\epsilon_{Bj}$ is found to be of the order of 1%, while the $SU(3)$ breaking parameter $\epsilon_{SU(3)}$ varies around a few percent, and cannot be determined with good accuracy from the available data. LO sets show similar features although with slightly higher $\chi^2$ and larger symmetry breaking parameters. The larger value of $\epsilon_{Bj}$ at LO is mostly related to order $\alpha_s$ corrections included at NLO but absent there.

In Table II, we also show at $Q^2=10$ GeV$^2$ the results for the first moment of each flavor distribution and the singlet $\delta\Sigma$, which is found to be between 0.2 and 0.15 and correlated to the value of $\delta G$.

Finally, in Table III we present the LO and NLO results for the first moments $\Gamma_1^{p,n}=\int dx\, g_1^{p,n}$ and the Bjorken sum rule evaluated at $Q^2=10$ GeV$^2$. The differences in the results obtained with the three sets are mostly due to the small $x$ extrapolation, in the case of the proton, and the lack of enough precise data, for the neutron targets.

## IV. COMBINED DATA

Having obtained all the information available from the inclusive data, we proceed to analyze also the antiquark densities, exploiting the semi-inclusive data. The constraining power of these asymmetries can be schemed in the following way. The production of positively (negatively) charged hadrons from proton targets is dominated by the convolution of

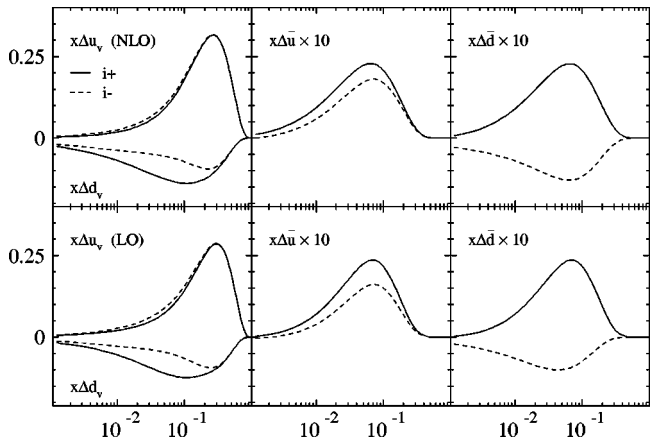


FIG. 3. NLO polarized densities from fits to combined data at $Q^2=10$ GeV$^2$.

$\Delta u$ ($\Delta d$) densities and ''favored'' fragmentation functions $D_1^\pi$, weighted with a factor of 4 (1) due to the electric charge

$$2g_{1p}^{\pi^+(-)}\sim\frac{4}{9}\Delta u\otimes D_{1(2)}^\pi+\frac{1}{9}\Delta d\otimes D_{2(1)}^\pi+\frac{4}{9}\Delta\bar{u}\otimes D_{2(1)}^\pi+\frac{1}{9}\Delta\bar{d}\otimes D_{1(2)}^\pi+\frac{2}{9}\Delta\bar{s}\otimes D_3, \tag{21}$$

where we can neglect the suppressed strange quark contributions, and in order to simplify the discussion, we have taken into account only final state $\pi$'s and within a LO expression.

Factoring out the $q+\bar{q}$ distributions which are almost completely fixed by the inclusive data we can write

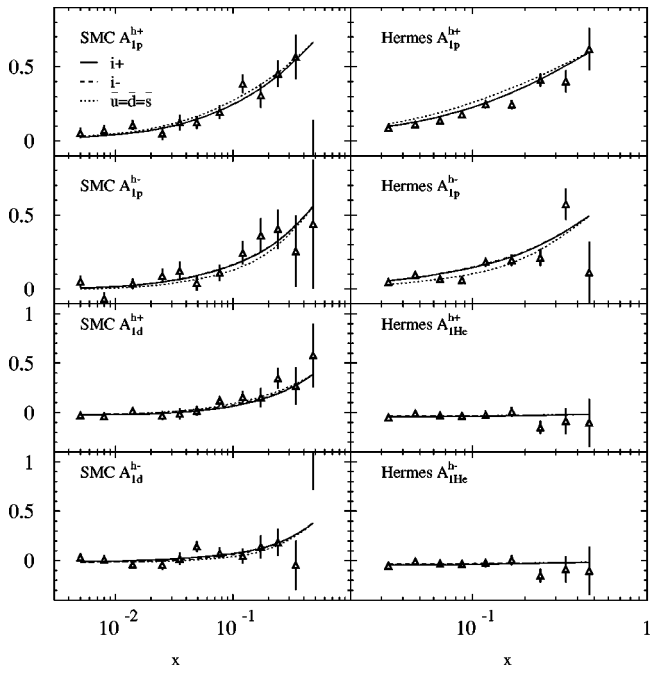


FIG. 4. Semi-inclusive asymmetries against NLO sets.

TABLE V. Coefficients for NLO total sets. Parameters marked by * are fixed by positivity constraints.

| Parameter | (i+) | (i−) | (ii+) | (ii−) | (iii+) | (iii−) |
|---|---|---|---|---|---|---|
| $\epsilon_{BJ}$ | −0.021 | −0.021 | −0.034 | −0.030 | −0.014 | −0.012 |
| $\epsilon_{SU(3)}$ | −0.002 | −0.001 | 0.056 | 0.045 | −0.064 | −0.068 |
| $\alpha_u$ | 0.873 | 0.877 | 0.921 | 0.918 | 0.936 | 0.933 |
| $\beta_u^*$ | 3.20 | 3.20 | 3.20 | 3.20 | 3.20 | 3.20 |
| $\gamma_u$ | 14.87 | 14.66 | 13.56 | 13.69 | 14.46 | 14.40 |
| $\delta_u$ | 1.06 | 1.06 | 1.00 | 1.00 | 0.97 | 0.97 |
| $\alpha_d$ | 0.460 | 0.460 | 0.474 | 0.465 | 0.446 | 0.443 |
| $\beta_d^*$ | 4.05 | 4.05 | 4.05 | 4.05 | 4.05 | 4.05 |
| $\gamma_d$ | 14.99 | 14.99 | 14.81 | 14.99 | 14.99 | 14.99 |
| $\delta_d$ | 1.65 | 1.67 | 1.66 | 1.66 | 1.62 | 1.63 |
| $N_s$ | −0.062 | −0.062 | −0.069 | −0.069 | −0.063 | −0.063 |
| $\alpha_s$ | 2.49 | 2.49 | 2.50 | 2.50 | 2.49 | 2.49 |
| $\beta_s$ | 10.00 | 10.00 | 10.16 | 10.16 | 10.32 | 10.32 |
| $N_{\bar{u}}$ | 0.065 | 0.046 | 0.059 | 0.044 | 0.055 | 0.042 |
| $\alpha_{\bar{u}}$ | 1.01 | 1.12 | 1.25 | 1.15 | 1.12 | 1.17 |
| $N_g$ | 0.25 | 0.27 | 0.40 | 0.40 | 0.7 | 0.7 |
| $\alpha_g$ | 1.5 | 1.5 | 1.5 | 1.5 | 1.5 | 1.5 |
| $\beta_g^*$ | 6.0 | 6.0 | 6.0 | 6.0 | 6.0 | 6.0 |
| $\chi^2$ | 330.52 | 330.00 | 330.98 | 330.22 | 332.31 | 331.64 |

$$2g_{1p}^{\pi+(-)} \sim \frac{4}{9}(\Delta u + \Delta\bar{u}) \otimes D_{1(2)}^{\pi} + \frac{1}{9}(\Delta d + \Delta\bar{d}) \otimes D_{2(1)}^{\pi} + \frac{1}{9}(\Delta\bar{d} - 4\Delta\bar{u}) \otimes (D_{1(2)}^{\pi} - D_{2(1)}^{\pi}), \tag{22}$$

where it is clear that the unconstrained component of both asymmetries is proportional to the same factor $(\Delta\bar{d} - 4\Delta\bar{u})$ but with opposite signs, and, regardless the values of $D_1$ and $D_2$, proton asymmetries are significantly more sensitive to $\Delta\bar{u}$ due to the difference in the electric charge factors.

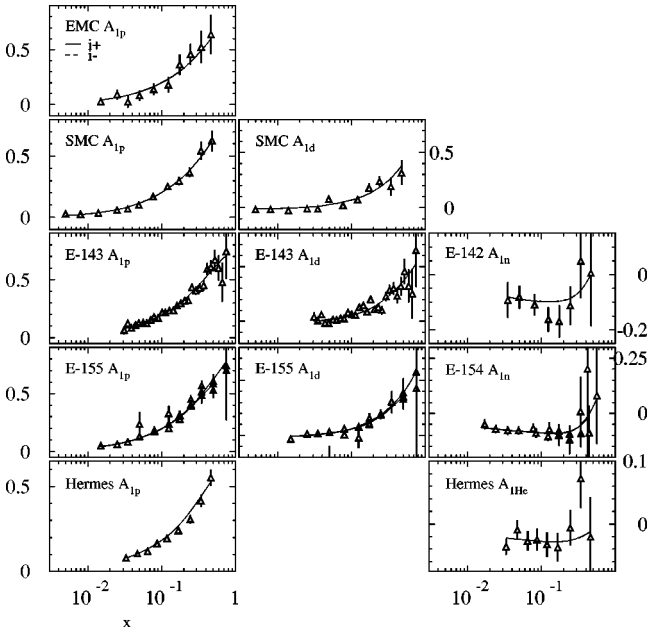


FIG. 5. Inclusive asymmetries against NLO sets.

Semi-inclusive asymmetries from neutron targets are proportional to a complementary combination of $\Delta\bar{d}$ and $\Delta\bar{u}$, and therefore are strongly dependent on $\Delta\bar{d}$. However, in practice, these last asymmetries have little impact on the analysis since they are heavily suppressed by the normalization coming from deuterium and helium unpolarized structure functions. Consequently, although $\Delta\bar{u}$ can be more easily pinned down, $\Delta\bar{d}$ densities are not very well constrained by the present data. Indeed we observe this feature in the global fits: the impact of $\Delta\bar{d}$ in terms of $\chi^2$ is very small and a large modification in its distribution can be easily balanced by a small modification of $\Delta\bar{u}$.

Taking into account the previous discussion, we parametrize $\Delta\bar{u}$ as in Eq. (14) (fixing $\alpha_{\bar{u}} = \alpha_{\bar{d}}$) but we restrict $\Delta\bar{d}$ to two somewhat extreme alternatives: one, labeled as ''+,'' in which $N_{\bar{u}} = N_{\bar{d}}$, and another, labeled as ''−,'' in which $N_{\bar{u}} = -N_{\bar{d}}$. These scenarios are motivated by expectations from different models that have been discussed in the literature. The first one ($\Delta\bar{d} = \Delta\bar{u}$ at $Q_0^2$) corresponds to the usual assumption about $SU(2)$ symmetry between light sea quarks. The second alternative ($\Delta\bar{d} = -\Delta\bar{u}$ at $Q_0^2$) breaks the $SU(2)$ symmetry at sea level along the lines of the statistical and chiral quark soliton models [6].

The results of allowing both the ''+'' and the ''−'' alternatives in the extended analysis that incorporates SIDIS data are presented in Table IV, where we show only the results associated with $\delta\bar{q}$ and $\delta q_v$ since those for the remaining parton densities are almost equal to the ''inclusive'' ones of Table II. This similarity can be easily understood

TABLE VI. Coefficients for LO total sets.

| Parameter | (i+) | (i −) | (ii+) | (ii−) | (iii+) | (iii−) |
|---|---|---|---|---|---|---|
| $\epsilon_{BJ}$ | −0.131 | −0.131 | −0.133 | −0.135 | −0.14 | −0.136 |
| $\epsilon_{SU(3)}$ | 0.071 | 0.067 | 0.032 | 0.047 | 0.036 | 0.039 |
| $\alpha_u$ | 0.768 | 0.777 | 0.766 | 0.768 | 0.77 | 0.767 |
| $\beta_u^*$ | 3.05 | 3.05 | 3.05 | 3.05 | 3.05 | 3.05 |
| $\gamma_u$ | 14.88 | 14.88 | 14.97 | 14.81 | 14.98 | 14.99 |
| $\delta_u$ | 1.64 | 1.64 | 1.69 | 1.69 | 1.69 | 1.69 |
| $\alpha_d$ | 0.5 | 0.499 | 0.502 | 0.52 | 0.532 | 0.527 |
| $\beta_d^*$ | 3.77 | 3.77 | 3.77 | 3.77 | 3.77 | 3.77 |
| $\gamma_d$ | 14.55 | 14.99 | 15.0 | 13.24 | 13.76 | 13.98 |
| $\delta_d$ | 1.68 | 1.75 | 1.69 | 1.69 | 1.69 | 1.69 |
| $N_s$ | −0.069 | −0.07 | −0.068 | −0.070 | −0.069 | −0.069 |
| $\alpha_s$ | 2.37 | 2.4 | 2.19 | 2.25 | 2.30 | 2.32 |
| $\beta_s$ | 11.42 | 11.42 | 11.42 | 11.42 | 11.42 | 11.47 |
| $N_{\bar{u}}$ | 0.060 | 0.043 | 0.058 | 0.042 | 0.056 | 0.041 |
| $\alpha_{\bar{u}}$ | 1.19 | 1.19 | 1.2 | 1.2 | 1.2 | 1.21 |
| $N_g$ | 0.35 | 0.35 | 0.6 | 0.6 | 0.7 | 0.7 |
| $\alpha_g$ | 1.8 | 1.78 | 1.8 | 1.8 | 1.8 | 1.8 |
| $\beta_g^*$ | 6.0 | 6.0 | 6.0 | 6.0 | 6.0 | 6.0 |
| $\chi^2$ | 336.24 | 335.54 | 334.19 | 334.03 | 334.26 | 333.69 |

taking into account the greater precision and the amount of these data. The parameters for the NLO and LO fits are presented in Tables V and VI, respectively.

In Fig. 3 we show the corresponding parton densities [only for sets (i+) and (i−), as the other ones are very similar], and in Figs. 4 and 5, the comparison with semi-inclusive and inclusive data, respectively. The lines in Figs. 4 and 5 interpolate, as usual, the results of the fit at the measured value of $Q^2$ of each data point, and for E-143 we show only the averaged data. For the experiments that provide only the values of $g_1$, we have computed the corresponding asymmetries with the procedure discussed above.

In Fig. 4 we include also an estimate for the semi-inclusive asymmetries computed using the parton distributions obtained in the analysis of inclusive data and assuming $SU(3)$ symmetry of the sea, i.e. $\Delta\bar{u}=\Delta\bar{d}=\Delta s$. As can be noticed, the differences are significant in the case of the Hermes data from proton targets, which completely dominates the fit of semi-inclusive data, whereas no distinction can be observed in the almost vanishing He asymmetries.

Furthermore, as can be expected from Eq. (22) the effect of a positive $\Delta\bar{u}$ distribution is to decrease (increase) the asymmetry for the production of positively (negatively) charged hadrons from proton targets with respect to the case of the $SU(3)$ symmetric result (which of course corresponds to a negative $\Delta\bar{u}$), as required by the experimental data.

As we mentioned, in the computation of the total $\chi^2$ values we properly take into account the correlations between SIDIS and inclusive data, finding that its main effect is just to increase slightly the total $\chi^2$ of the fits.

Notice that the six sets of parton densities in Table IV have positive $\Delta\bar{u}$ densities; however, their sizes are still correlated to the choice for $\Delta\bar{d}$. This is in agreement with the discussion below Eq. (22), since the correlation between $\Delta\bar{u}$ and $\Delta\bar{d}$ is such that $(\Delta\bar{d}-4\Delta\bar{u})$ remains roughly the same for all sets.

It should be noticed also that even in the case of $SU(2)$-symmetric alternatives (labeled as ''+''), there are small differences between the first moment of the $\Delta\bar{u}$ and $\Delta\bar{d}$ at $Q^2=10$ GeV$^2$, notwithstanding they are set to be equal at the initial scale $Q_0^2$. The difference comes from the fact that these distributions evolve differently at NLO due to both the appearance of different non-singlet quark splitting func-

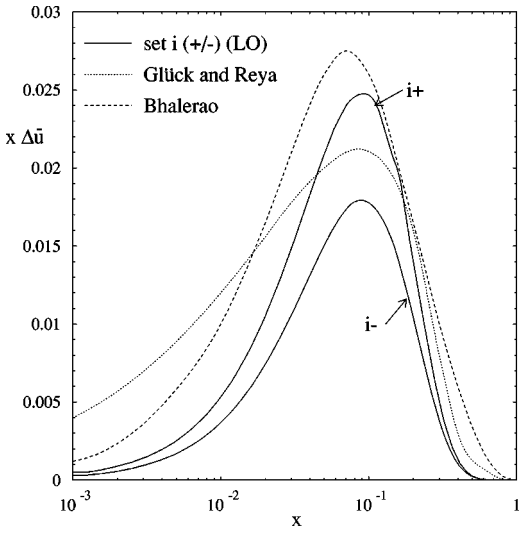


FIG. 6. $x\Delta\bar{u}$ (set i) at $Q^2=1$ GeV$^2$ compared to the predictions in Ref. [6].

TABLE VII. Coefficients for LO and NLO inclusive sets.

| | NLO | | | LO | | |
|---|---|---|---|---|---|---|
| Parameter | (i) | (ii) | (iii) | (i) | (ii) | (iii) |
| $\epsilon_{BJ}$ | −0.015 | −0.018 | −0.0025 | −0.126 | −0.126 | −0.126 |
| $\epsilon_{SU(3)}$ | −0.003 | 0.037 | −0.063 | 0.016 | 0.018 | 0.009 |
| $\alpha_u$ | 0.876 | 0.915 | 0.928 | 0.766 | 0.77 | 0.771 |
| $\beta_u^*$ | 3.2 | 3.2 | 3.2 | 3.05 | 3.05 | 3.05 |
| $\gamma_u$ | 14.53 | 13.37 | 14.38 | 14.99 | 14.94 | 14.84 |
| $\delta_u$ | 1.06 | 1.0 | 0.97 | 1.66 | 1.68 | 1.68 |
| $\alpha_d$ | 0.46 | 0.47 | 0.43 | 0.471 | 0.477 | 0.49 |
| $\beta_d^*$ | 4.05 | 4.05 | 4.05 | 3.77 | 3.77 | 3.77 |
| $\gamma_d$ | 14.99 | 14.85 | 14.66 | 15.0 | 14.98 | 14.97 |
| $\delta_d$ | 1.675 | 1.66 | 1.55 | 1.72 | 1.68 | 1.68 |
| $N_s$ | −0.062 | −0.069 | −0.064 | −0.065 | −0.068 | −0.069 |
| $\alpha_s$ | 2.49 | 2.5 | 2.49 | 2.38 | 2.38 | 2.38 |
| $\beta_s$ | 10.0 | 10.16 | 10.32 | 11.42 | 11.42 | 11.42 |
| $N_g$ | 0.25 | 0.4 | 0.7 | 0.35 | 0.59 | 0.7 |
| $\alpha_g$ | 1.5 | 1.5 | 1.5 | 1.8 | 1.8 | 1.75 |
| $\beta_g^*$ | 6.0 | 6.0 | 6.0 | 6.0 | 6.0 | 6.0 |
| $\chi^2$ | 228.66 | 228.69 | 230.33 | 237.55 | 236.1 | 236.44 |

tions and the non-zero value of $\Delta u_v - \Delta d_v$. Therefore the $SU(2)$ symmetry in the light sea sector is perturbatively broken, as happens in the unpolarized case, but the size of this breakdown is small compared to what is required by the SIDIS data. Notice that this effect is absent in the LO case, where there is only one $qq$ splitting function.

It is worthwhile mentioning that the slight differences in the $\chi^2$ between ''+'' and ''−'' sets are comparable to the uncertainties of the fitting procedure, such as the use of slightly different parametrizations for the initial distributions, the arbitrariness in choosing the initial scale $Q_0^2$, or other external constraints. For this reason, we can conclude that $\Delta\bar{d}$ densities are not well constrained by the present data, and the slight differences in $\chi^2$ fail to justify a definite statement about isospin symmetry at the sea quark level. At variance with $SU(2)$, $SU(3)$ symmetry in the sea seems to be clearly broken in the sense that fits prefer $\Delta\bar{u}$ and $\Delta\bar{s}$ with opposite polarization.

In order to try to quantify uncertainties in the spin dependent distributions, specifically, those introduced by the assumptions done about the fragmentation functions, we have varied the parameter $a$ of Eq. (9), which was fixed to 1 in the previous fits, from 0.75 to 1.25. Doing this, we find that this variation produces only negligible changes in the $\Delta\bar{u}$ distribution, which is explained by a large cancellation of its effect in the rate of polarized and unpolarized SIDIS structure functions. Of course, this by no means constitutes an exhaustive study of the related uncertainties, but it makes us more confident about the sensitivity of our results to some unavoidable assumption.

Although for the time being we do not intend to perform a comprehensive analysis of other uncertainties involved in the extraction of the parton distributions presented here, a problem which is far from being solved even in the unpolarized case [30], we find it reasonable to claim that the present data give a clear signal of a positive $\Delta\bar{u}$ distribution. Actually, we have found it to be impossible to produce parton densities constraining $\Delta\bar{u}$ to be negative, unless we allow an increase in the $\chi^2$ value of the order of 5% (about 10–20 units), showing the sensitivity of the semi-inclusive data.

Noticeably, most of the available theoretical calculations [6] predict a positive $\Delta\bar{u}$ distribution. In Fig. 6 we show our LO results for $\Delta\bar{u}$ from fits (i+) and (i−) compared to the prediction of Glück and Reya and the one of Bhalearo [6] at $Q^2=1$ GeV$^2$. As can be seen, there is a reasonable agreement between those predictions and our results in the kinematical region covered by the Hermes semi-inclusive data (i.e. $0.4>x>0.03$), at least within the expected uncertainties in the extracted distributions. Of course, there is no experimental evidence yet at smaller values of $x$, so our results just provide an extrapolation in that region. The same models predict also a negative $\Delta\bar{d}$; however, as stated before, global fits still do not discriminate a preferred alternative to compare with.

At this point it is worth comparing our results to the ones reported by the Hermes Collaboration in Ref. [10]. There, no definitive sign for $\Delta\bar{u}$ is found. Besides the fact that we take into account the correct $Q^2$ evolution of the distributions both up to LO and NLO accuracy, whereas Hermes uses naive parton model expressions assuming $Q^2$ independence of the asymmetries, the main difference comes from the fact that we perform the fit to *all* available inclusive and semi-inclusive data (not only the one coming from Hermes), and that we do not impose any constraint on $\Delta\bar{q}$ distributions. In the Hermes analysis sea quark distributions are constrained to have the same sign, and taking into account that the strange quark distribution $\Delta s$ is found to be negative already

from the inclusive data, this constraint introduce a strong bias against the $SU(3)$ breaking in the sea as found in our analysis.

## V. CONCLUSIONS

The main conclusion of this analysis is that semi-inclusive spin dependent data available today are not only in perfect agreement with inclusive data with regard to the extraction of polarized parton densities, but constitute a very useful tool to investigate polarization among sea quarks. Specifically, we have found that SMC and Hermes data show a clear preference for parton distributions with ''up'' antiquarks polarized along the nucleon spin and strange quarks with the opposite polarization.[3]

Regarding ''down'' antiquarks, although the global fits attain marginally lower values of $\chi^2$ when these are polarized in opposition to ''up'' antiquarks, the differences are so small that we conclude that the data are unable to discriminate between the different alternatives.

The agreement between polarized parton densities obtained from global fits and the constraints coming from hyperon decay data is particularly good in NLO, with departures of the order of a few percent, but larger for LO sets, partly due to higher order QCD effects.

[3]A FORTRAN code containing a parametrization of our distributions is available upon request.

## ACKNOWLEDGMENTS

We thank S. Kretzer for providing us with his routines for fragmentation functions and A. Brüll for kindly providing us Hermes data before publication. D.dF. was partially supported by the EU Fourth Framework Program ''Training and Mobility of Researchers,'' Network ''Quantum Chromodynamics and the Deep Structure of Elementary Particles,'' contract FMRX-CT98-0194 (DG 12–MIHT). R.S. was partially supported by CONICET, ANPCyT, and Fundación Antorchas.

[1] B. Lampe and E. Reya, Phys. Rep. **332**, 1 (2000); E. Leader *et al.*, *ibid.* **261**, 1 (1995).
[2] M. Glück, E. Reya, M. Stratmann, W. Vogelsang, Phys. Rev. D **53**, 4775 (1996); T. Gehrmann and W. J. Stirling, *ibid.* **53**, 6100 (1996); K. Abe *et al.*, Phys. Lett. B **405**, 180 (1997); C. Bourrelly *et al.*, Prog. Theor. Phys. **99**, 1017 (1998); G. Altarelli *et al.*, Acta Phys. Pol. B **29**, 145 (1998).
[3] D. de Florian, O. Sampayo, and R. Sassot, Phys. Rev. D **57**, 5803 (1998).
[4] L. E. Gordon, M. Ghostasbpour, and G. P. Ramsey, Phys. Rev. D **58**, 094017 (1998); E. Leader, A. V. Sidorov, and D. B. Stamenov, *ibid.* **58**, 114028 (1998); Y. Goto *et al.*, *ibid.* **62**, 034017 (2000); J. Bartelski and S. Tatur, hep-ph/0004251.
[5] D. K. Ghosh, S. Gupta, and D. Indumati, Phys. Rev. D **62**, 094012 (2000).
[6] M. Wakamatsu and T. Watabe, Phys. Rev. D **62**, 017506 (2000); B. Dressler *et al.*, Eur. Phys. J. C **14**, 147 (2000); M. Glück and E. Reya, Mod. Phys. Lett. A **15**, 883 (2000); R. S. Bhalerao, hep-ph/0003075.
[7] T. Morii and T. Yamanishi, Phys. Rev. D **61**, 057501 (2000).
[8] D. de Florian, C. A. García Canal, and R. Sassot, Nucl. Phys. **B470**, 195 (1996).
[9] SMC Collaboration, B. Adeva *et al.*, Phys. Lett. B **420**, 180 (1998).
[10] Hermes Collaboration, K. Ackerstaff *et al.*, Phys. Lett. B **464**, 123 (1999); B. E. Tipton, Ph.D. thesis, Massachusetts Institute of Technology, 1999.
[11] D. de Florian and R. Sassot, Phys. Rev. D **51**, 6052 (1995).
[12] T. Gehrmann, Nucl. Phys. **B534**, 21 (1998).
[13] D. de Florian *et al.*, Phys. Lett. B **389**, 358 (1996).
[14] R. D. Field and R. P. Feynman, Nucl. Phys. **B136**, 1 (1978).
[15] EMC Collaboration, M. Arneodo *et al.*, Nucl. Phys. **B321**, 541 (1989); J. J. Aubert *et al.*, Phys. Lett. **160B**, 417 (1985); P. Geiger, Ph.D. thesis, Ruprecht-Karls-Universität, 1998.
[16] E143 Collaboration, K. Abe *et al.*, Phys. Lett. B **452**, 194 (1999).
[17] M. Glück, E. Reya, and A. Vogt, Eur. Phys. J. C **5**, 461 (1998).
[18] S. Kretzer, Phys. Rev. D **62**, 054001 (2000).
[19] J. D. Bjorken, Phys. Rev. **148**, 1467 (1966).
[20] J. Ellis and R. L. Jaffe, Phys. Rev. D **9**, 1444 (1974).
[21] EMC Collaboration, J. Ashman *et al.*, Nucl. Phys. **B328**, 1 (1989).
[22] SMC Collaboration, B. Adeva *et al.*, Phys. Rev. D **58**, 112001 (1998).
[23] E143 Collaboration, K. Abe *et al.*, Phys. Rev. D **58**, 112003 (1998).
[24] E155 Collaboration, P. L. Anthony *et al.*, Phys. Lett. B **463**, 339 (1999); G. S. Mitchell, Ph.D. thesis, University of Wisconsin-Madison, SLAC Report No. 540, 1999.
[25] E142 Collaboration, P. L. Anthony *et al.*, Phys. Rev. D **54**, 6620 (1996).
[26] E154 Collaboration, K. Abe *et al.*, Phys. Rev. Lett. **79**, 26 (1997); Phys. Lett. B **405**, 180 (1997).
[27] D. de Florian, S. Frixione, A. Signer, and W. Vogelsang, Nucl. Phys. **B539**, 455 (1999); D. de Florian and S. Frixione, Phys. Lett. B **457**, 236 (1999).
[28] S. Frixione and W. Vogelsang, Nucl. Phys. **B568**, 60 (2000).
[29] I. Bojak and M. Stratmann, Nucl. Phys. **B540**, 345 (1999); I. Bojak, hep-ph/0005120.
[30] R. Brock *et al.*, hep-ph/0006148.